Medical & Biological Engineering & Computing

doi: 10.1007/s11517-015-1309-4

Available at http://link.springer.com/article/10.1007/s11517-015-1309-4

Using Visual Cues to Enhance Haptic Feedback for Palpation on Virtual Model of Soft Tissue

Min Li · Jelizaveta Konstantinova · Emanuele L. Secco · Allen Jiang · Hongbin Liu · Thrishantha Nanayakkara · Lakmal D. Seneviratne · Prokar Dasgupta · Kaspar Althoefer · Helge A. Wurdemann

the date of receipt and acceptance should be inserted later

Abstract This paper explores methods that make use of visual cues aimed at generating actual haptic sensation to the user, namely pseudo-haptics. We propose a new pseudo-haptic feedback based method capable of conveying 3D haptic information and combining visual haptics with force feedback to enhance the user's haptic experience. We focused on an application related to tumor identification during palpation and evaluated the proposed method in an experimental study where users interacted with a haptic device and graphical interface while exploring a virtual model of soft tissue, which represented stiffness distribution of a silicone phantom tissue with embedded hard inclusions. The performance of hard inclusion detection using force feedback only, pseudo-haptic feedback only, and the combination of the two feedbacks were compared with the direct hand touch. The combination method and direct hand touch had no significant difference in the detection results. Compared with the force feedback alone, our method increased the sensitivity by 5%, the

M. Li
School of Mechanical Engineering, Xi'an Jiaotong University, Xi'an 710049, Shaanxi, China.
Tel.: +862982663707
Fax: +862982664257
E-mail: min.li@mail.xjtu.edu.cn

J. Konstantinova · E. L. Secco · A. Jiang · H. Liu · T. Nanayakkara · L. D. Seneviratne · K. Althoefer · H. A. Wurdemann
Department of Informatics, Kings College London, London, WC2R 2LS, UK.

E. L. Secco
Department of Mathematics and Computer Science, Hope University, Liverpool, UK.

L. D. Seneviratne
College of Engineering, Khalifa University of Science, Technology and Research, Abu Dhabi, U.A.E.

P. Dasgupta
Medical Research Council (MRC) Centre for Transplantation, King's College London, Kings Health Partners, Guys Hospital, London SE1 9RT, UK.

positive predictive value by 4%, and decreased detection time by 48.7%. The proposed methodology has great potential for robot-assisted minimally invasive surgery and in all applications where remote haptic feedback is needed.

Keywords Haptic feedback · Pseudo-haptic feedback · Rigid tool-soft tissue interaction · Tumor identification

1 Introduction

Haptic Feedback (HF) creates a sensation of touch when a user interacts with a remote object. Most current HF systems provide graphical feedback of the contact area through computer graphics, and single-point Force Feedback (FF) through a haptic interface, such as actuated joysticks or input devices like the PHANToM Omni [10]. Such HF techniques greatly distort the representation of object properties [11].

Pseudo-haptics is a feedback method, which creates the illusion of actual FF through appropriately adapted visual cues [14] such as active cursor displacements [22]. The advantage of Pseudo-Haptic Feedback (PHF) is that it generates virtual forces through visual feedback only, thus no extra hardware beyond the standard computer systems and associated display screens is needed. In another word, no FF devices are needed for PHF. PHF can be easily combined with other HF techniques without affecting the control performance of the system [8]. PHF has been used to express haptic properties such as friction, spring stiffness, mass, softness induced by grasping motion, and texture [9,12,13,15]. Pseudo-haptic texture techniques have also been implemented in medical training for anesthesia [2]. Moreover, two-dimensional PHF has been used in experimental studies for soft tissue stiffness simulation and abnormality localization [16]. Most current PHF techniques are applied to express one-dimensional [14] or two-dimensional haptic information [8,15].

To the best of our knowledge, our study is the first time that PHF is used to express three-dimensional haptic information. Moreover, the combination of PHF with other technologies looks promising: Hachisu et al. have successfully combined PHF with visual jitters and tactile vibrations and they claim the combination of cues from the visual and tactile modalities strengthened the perception [8]. Some theoretical research has been conducted to investigate the domination perception modality between visual and haptic feedback cues [4,13,22]. It has been shown that humans integrate visual and haptic information in a statistically optimal fashion that is similar to a maximum-likelihood integrator [4]. This research apart, the benefits of a PHF and FF combination have not been studied in detail yet, especially for soft tissue haptic perception.

Compared to the conventional minimally invasive surgery, minimally invasive robotic surgery has augmented the distal dexterity of the surgical tools and enabled surgeons to carry out surgical procedures on an intuitive user interface. However, surgical robotic systems cannot yet convey the quality of haptic feedback that manual organ palpation provides [6]. Tumor nodules are typically stiffer than the surrounding tissue like the kidney, the liver, or

the breast tissues [21,30]. In our previous research [17], a virtual-environment tissue model was created based on the reconstructed surface of an artificial soft-tissue organ using a Kinect depth sensor and the organ's stiffness distribution acquired during rolling indentation measurements on a phantom tissue sample. With this tissue model, users can explore the stiffness distribution in the virtual environment with the aid of a haptic device. However, the proposed palpation method required more time for the users to detect the hard nodules than manual palpation [17].

In this paper, a PHF method is combined with FF to establish whether the combination of the two cues can strengthen the end-user haptic perception of the interaction between a rigid tool and a soft tissue and whether it can reduce the time required of nodule detection during palpation. This combination feedback method is applied to the problem of the identification of hard inclusions representing tumors inside a soft tissue. Here, a soft tissue model for palpation is created based on rolling indentation [18,19] tests on a soft tissue silicone phantom. This paper has the following contributions:

1) Generating a haptic tissue model that is capable of representing tissue stiffness distribution of the examined soft tissue;

2) Presenting three-dimensional haptic information using PHF;

3) Augmenting FF with PHF in an experimental and validation study.

2 Methods

2.1 Overview

The proposed method aims at providing HF of the interaction between a rigid tool and a soft tissue within a virtual environment. Fig. 1 depicts the method flow chart: a deformable virtual soft tissue model was developed based on a mechanical characterization of a silicone phantom tissue; then our method allowed the experience of a reaction force via both PHF and FF while exploring the tissue and identifying embedded hard inclusions.

In the following paragraphs, the description of the soft tissue computer model, visualization of soft tissue deformation, PHF, FF, and combination of the two feedbacks are reported.

2.2 Soft tissue virtual model

As various evaluation studies demonstrated [18,34], a single probe might be enough to substitute multi-fingered palpations. In our method a rolling indentation probe [18,19], which was attached to a robot arm, was used to non-graspingly palpate the soft tissue to obtain the stiffness distribution. In order to study the proposed haptic concepts and their capability to convey haptic force information to humans, a realistic soft tissue computer model was implemented to mimic the tissue deformation during this non-grasping palpation.

The model was based on previous experimental acquisitions from a silicone block. According to the 2003 American joint committee on cancer staging, T1 stage tumors are 20 mm or less in greatest dimension [35]. The silicone block was a $120 \times 120 \times 25\ mm^3$ rectangular cuboid containing three differently-sized spherical hard nodules (A: 10 mm, B: 8 mm, and C: 6 mm in diameter). The nodules were buried at a depth of 6 mm measured from each spheres top to the silicone surface. The phantom tissue was made from RTV6166 (ratio 3 : 7, Young's modulus 15.3 kPa), which is commonly used to fabricate artificial visceral tissue samples [19,27]. The nodules were made from a rubber eraser STAEDTLER Mars plastic 526 50 (Young's modulus about 1.59 MPa). The ratio of Young's modulus of the hard nodules to the silicone block was about 104 which was within the range of the ratios of elastic modulus of cancerous breast tissues to fat tissue (ranging from 4 to 124) reported in [30]. 59 straight rolling trajectories (121 mm long and parallel to the x-axis with an interval of 4 mm along the y-axis between every two trajectories) were defined. The speed was set at 30 mm s^{-1}. Indenter-silicone interaction forces were recorded with a Nano 17 (ATI technologies) force/torque sensor (resolution: 0.003 N). Normal and horizontal reflected forces were recorded at 100 Hz. The experiments were repeated at different indentation depths varied between 2 and 7 mm at intervals between paths of 1 mm. The indentation depth was kept constant during one scan. Thus, six 159×59 normal and horizontal force matrices were created, which allowed us to obtain stiffness distribution maps for the whole silicone block surface to be used for our experimental studies.

2.3 Visualization of soft tissue deformation

Mass-spring models and finite element modeling are two standard techniques used to simulate soft tissue deformation during rigid-tool/soft tissue interaction on the soft tissue computer model [24]. Both techniques have some disadvantages: mass-spring models ignore the impact of the indenter diameter on the soft tissues deformation while the use of finite element modeling cannot usually achieve real-time performance due to high computational complexity [27].

Here, we propose a real-time deformable model for hyperelastic materials. Our model considers the influence of the indenter diameter based on a predefined finite element model. We have tested the influence of different hyperelastic material properties on the relationship between the curvature of the soft tissue surface and other influencing factors (indentation depth and diameter of indenter). In particular, we varied the indenters diameter between 6 and 10 mm and investigated different material properties including shear modulus μ, locking stretch λ_m and mass density (silicone (RTV6166 gel): μ = 4.98 kPa, λ_m = 1.05, σ= 980 kg m^{-3}; porcine kidney: μ = 1.85 kPa, λ_m = 1.05, σ = 800 kg m^{-3}; material properties were obtained from uniaxial compression tests [19]). We have conducted three-dimensional finite element modeling of soft tissue indentation based on hyperelastic Arruda-Boyce equa-

tions. The tissue surface was lubricated, thus the contact between the indenter and simulated soft tissue can be defined as frictionless. The posterior part of the soft tissue was defined as fixed. The results have shown that the investigated different hyperelastic material properties have virtually no impact on the deformation curvature of the soft tissue surface (see Fig. 2). In Fig. 2, although the difference between the two curvatures was comparatively larger in the case of indentation depth -2r when an indenter with a diameter of 10 mm was used, the difference was still less than $r/100$ compared to the radius of the indenter r. Thus, one geometrical deformable soft tissue model applies to those hyperelastic materials we examined. In the scope of this research, we assume that it can be applied to any hyperelastic material. Specifically, it refers to tissues like kidney, liver and breast tissues in our paper.

Employing the above geometrical deformable soft tissue model, we proposed to graphically display the silicone block surface by using a mesh of connected triangles, whose vertices form a graph of nodes (see Fig. 3(a)). For a node i at the center of an indentation (caused by a spherical indenter), its perpendicular vertex was updated as a function of the indentation depth. The perpendicular vertices of other affected nodes on the mesh (such as node i-1, i+1, i-x and i+x, in Fig. 3(a)) were then updated as a function of the distance between the node i and the soft tissue surface deformation presented in Fig. 3 (c), where the indentation depth d_A was defined as the distance between the soft tissue surface and the largest displacement point (bottom point of the indenter). According to this modeling method, the indentation depth was then divided into four ranges, where the demarcation points are $(2\text{-}\sqrt{3}) \cdot r/2$, r, and $2r$ for the (a), (b), (c), and (d) cases, respectively (see Fig. 3 (c)). As the indentation depth increases, the number of the affected vertices of the triangle also increases, and thus, tissue deformation increases(see Fig. 3(b)). Therefore, the depths of the subsequent neighboring points d_B, d_C, d_D, d_E, d_F, d_G, which were at a distance of $r/2$ apart − were defined as functions of d_A. It is important to note that, for soft tissues with curved surfaces, the aforementioned model can be accepted under the assumption that the relevant area around the indentation center is planar.

2.4 Pseudo-haptic feedback and rigid-tool / soft tissue interaction

During palpation, human operators use fingers to slide and press the surface of the soft tissue to perceive its stiffness. Generally, if the indentation depth increases during this exploration procedure, the reflecting force also increases. In particular, if the finger approaches a relatively hard area of a soft tissue with buried hard nodules beneath the surface, then the reaction forces (the lateral f_h and normal forces f_n) increase.

Here, a PHF method, which can convey 3D haptic information, was implemented to simulate a touch exploration procedure performed by the operator with the use of a remote stylus or haptic device. The relationship between the master movement (i.e. the operator action) and the movement of the slave

avatar (i.e. the cursor displacement) was introduced in our PHF method. Precisely, an illusion of a resistance to motion occurs when the cursor's speed becomes slower than the user's expectation, returning the impression of a stiffness increase. To create this illusion, the relative movement speed of the cursor can be appropriately reduced or increased with respect to the speed of the movement at the user's input console such as a joystick or a pen-like input stylus (see Fig. 4 (a)).

Since the proposed method operates in real time (i.e. the user's input occurs at the same time as the cursor on the display is being updated), the cursor displacement (d) is varied in a function of the corresponding displacement at the user input device (D), according to a cursor/user input ratio ($R = d/D$) ratio (see Fig. 4 (a)). Whenever the end-user moves the input stylus (a pen-like device located at the end effecter of the operator input device) towards a hard area (hard nodule in a soft tissue) across a certain distance (D), the cursor/user input ratio R is reduced accordingly. A default ratio R_o is introduced to characterize the ratio between the two displacements in the object's default soft regions. Hence, in order to make the user experience the illusion of a resistance to the input motion, when the subject approaches a harder area (a hard nodule in a soft tissue, e.g. a tumor in a soft tissue organ) R is reduced to a smaller value $R_m (R_m < R_o)$, and as a consequence, the modified cursor displacement d_m becomes smaller than the default cursor displacement d_o ($d_m = R_m \cdot D$, $d_o = R_o \cdot D$). Thus, virtual forces are perceived through visual perception since the user experiences an imaginary force against the motion direction provided at the input console. After the hard nodule has been passed, the default cursor/user input ratio R_o is applied again. Specifically, the modified cursor/user input ratios at normal and tangential directions (R_n and R_h) are defined as follows:

$$\Delta f_n = f_n - f_{nl}, \tag{1}$$

$$R_n = R_0/(f_n + 1), \tag{2}$$

$$R_h = R_0/(f_h + 1), \tag{3}$$

where the reaction force values (tangential reaction force f_h and normal force f_n) are acquired from the force matrices obtained by physically exploring the surface with the rolling indentation: f_{hl} is the normal reaction force value at the previous cursor position; R_n is the modified normal cursor/user input ratio and R_h is the modified horizontal cursor/user input ratio. In summary, the cursor displacement distance is modified according to the set of rules reported within Table 1.

2.5 Force feedback

FF is a common way to convey haptic perception. A PHANToM Omni device, which can provide 3-DOF tracking of stylus motion, has been introduced to allow the operator to provide input during the PHF and, at the same time, to convey 3D FF to the subject while exploring the soft tissue. The FF calculation

has been implemented and based on the indentation depth caused by the indenter avatar displacement over the soft tissue model. The indenter avatar displacement is controlled by the effective displacement of the stylus of the haptic device. The force calculation is based on a look-up table of measured object deformation/force pairs. This method assumes a constant palpation velocity of the soft tissue surface.

In practice, the current cursor position and the previous cursor position were read by the program first; in case of a contradiction event between the cursor position and the original contour of the soft tissue, the horizontal and normal force values were acquired through a look-up table. Then the projection of the vector pointing from the previous cursor position P_l to the current cursor position P_c on the horizontal plane V_h was used to represent the horizontal force direction, namely:

$$V_h \equiv \overrightarrow{P_l P_c}, \tag{4}$$

where P_l (x_l,y_l) and P_c (x_c,y_c) were defined as the previous and current cursor positions, respectively. The horizontal component vector of the force direction V_h was then transformed to a unit vector with the same direction as the horizontal component vector. The horizontal force was generated along the same direction of the unit vector of horizontal force direction:

$$\widehat{V_h} = \frac{V_h}{|V_h|}. \tag{5}$$

Finally, the normal reaction force was not generated when the indentation depth decreased. When the force in the look-up table exceeded the maximum force (3.3 N) of PHANToM Omni, the force was set to 3.3 N.

2.6 Combined pseudo-haptic feedback and force feedback

With the aim to further improve on what can be achieved in an HF system, a new method was introduced which combines PHF with FF in order to enhance the haptic perception of the user while interacting with soft tissue and embedded hard inclusions. Since the two mechanisms, namely the PHF and FF, are diverse, they can be easily combined and will not technically have an adverse effect on each other [8]. FF is fed to the hand of the user through a haptic device, while the PHF information is fed to the user via a graphical interface (see Fig. 4 (b)). Therefore, the force perception of the user is the results of a combination of sensations based on the proprioceptive and visual sensors of the subject.

2.7 Experimental evaluation for hard nodule identification

User experience with interactive virtual environments can be characterized by three indicators including how well the user feels when he/she interacts with the system, how well the user performs an interactive task within the

particular virtual environment, and how long the task takes for the user to complete it. An experimental validation study aimed at measuring the benefits of the proposed method was performed. The experiment considered four tests in order to (a) define the efficiency of the proposed method, (b) explore the advantages or shortcomings of using a combined PHF and FF method, (c) evaluate the feasibility of this method as a replacement for manual palpation (direct touch by hand).

Twenty participants (age range: 23−42) were involved in the trials: 6 women and 14 men. One had palpation experience and one was left-handed. The following four tests were performed by each subject in a pseudo-random fashion. For each test, the same stiffness distribution was used, but the orientation of the silicone block and silicone block model was changed randomly from time to time to ensure that the participants did not learn the locations of the nodules from the tests conducted earlier. During the test a stopwatch was used in order to measure the time required by the subject to detect the nodules. The instrument allowed a precision of the time measurement of ± 1 s.

Test 1: Manual Palpation

At first, participants were asked to do an acquaintance trial run by palpating transparent silicone blocks containing or not containing visible hard inclusions inside. During the real tests, participants were asked to manually palpate the silicone block with hard nodules embedded at unknown locations covered by a black plastic sheet. Then they were asked to determine at which locations they believed to have sensed hard nodules. The time needed for the detection was recorded until they thought they had found all the nodules.

Test 2: PHF

Participants were again asked to do a practice run with visible hard nodule locations. Then, they were asked to palpate the virtual soft tissue block with the embedded hard nodules (that are invisible to the participant) inside using only PHF, and to indicate the positions of the hard nodules they believed to have found. The time taken to detect all nodules was recorded.

Test 3: FF

The procedure was the same as in Tests 1 & 2. The subjects were asked this time to perform palpation relying on FF only and then to indicate the different positions where they believed to have found hard inclusions. Again, the time needed to detect nodules was recorded.

Test 4: Combination of PHF and FF

A practice run of the test was first conducted. Then, participants were asked to palpate the virtual soft tissue block with hidden nodules by using the combined feedback method and then asked to indicate the different positions where they believed to have found hard inclusions. The time needed to detect all nodules was recorded for each participant.

At the end of the four tests, every participant was asked whether there was any difference in perception with combined feedback versus FF alone.

The sensitivity Se [1], which relates to the test's ability to identify positive results, and the Positive Predictive Values PPV [5] were used as measures of the performance of the palpation methods. Wilson score intervals [32], which

have good properties even for a small number of trials (less than 30) and/or an extreme probability, were calculated for sensitivity at a 95% confidence level. The measures of the performance of the palpation methods were compared in pairs. It was conducted by comparing the observed probabilities (p_1 and p_2) with a combined interval (CI), which was calculated using the method described in [31]. If $p_1 - p_2 > CI$, there is a significance between the two tests. Wilcoxon signed-rank test [3,31] was used to compare the time consumed by each pair of feedback method modes. Using this test, one can decide whether the sample size distributions are identical without checking the normal distribution [3].

3 Results

Fig. 5 (a) presents the nodule detection sensitivities of nodule A, B, and C obtained by using different palpation techniques. In general, there was a positive correlation between the detection sensitivities and nodule size − bigger nodules had higher detection sensitivities (mX represents the overall detection sensitivity of nodule X: $mA = 91.3\%$, $mB = 76.3\%$, $mC = 53.75\%$). Compared with FF only, the proposed combination technique improved the sensitivity Se of the middle sized nodule B dramatically from 75 to 90%, but reduced the sensitivity Se of the largest nodule slightly from 95 to 90%. This indicates that the combined technique was particularly suitable for detecting middle-sized nodules.

Fig. 5 (b) presents the overall nodule detection sensitivity of each feedback method. The best Se was achieved with the combined technique utilizing both PHF and FF (83.3% with 95% confidential interval 71.9 − 90.7%). The technique using only pseudo-haptic feedback had a sensitivity Se of 50% (37.7 − 62.3%) overall. The performance of FF was better with a sensitivity Se of 78.3% (66.3 − 86.9%).

Fig. 5 (c) presents the PPV. Compared to PHF and FF, PPV of the combination method was larger.

Sensitivities Se and Positive Predictive Values PPV were compared in pairs. Table 2 shows the test results. While manual palpation showed significant better performance than FF with regards to PPV, the combination method showed no significant difference from manual palpation with regards to both Se and PPV.

Fig. 5 (d) depicts the difference in the time taken to detect the hard nodules with each technique. It is important to outline that the detection time was shortest when using the combined technique. The time consumed was even shorter than for manual palpation (73.6 s *vs.* 106.2 s). Table 2 shows the Wilcoxon signed-rank test results. The significance level 0.05 was checked. The combination method needed significantly less time than the FF and PHF tests and had no significant difference from the gold standard, i.e. manual palpation (see Table 3).

The majority of the participants (n = 16, 80%) surveyed stated that the perception using the combination method was enhanced when compared to the perception from FF alone.

4 Discussion

Although PHF on hard nodule detection was the least effective method among the experimentally investigated methods, PHF has been proven to be able to express haptic information effectively in rigid tool-soft object interaction in virtual environments. PHF provides a low-cost method to simulate soft object stiffness and hard inclusions and can be useful in applications where haptic sensations are needed and where budgets are limited. For instance, video game applications may rely on PHF with no need for expensive haptic devices.

In regards to medical applications the proposed technique presents a departure from the empirical mathematical models widely used in medical simulators. Instead, it uses a model based on real organ experimental data − a palpation simulation based on data from an indentation probing test of a silicone block. This model presented a stiffness behavior similar to the behavior of the tested silicone block and the applied methodology could be easily extended to real organs palpation. Following the preliminary validation of the proposed concept reported in this paper, different tissue characteristics and shapes, as well as participants with different expertise can be addressed in further validation. For this reason, ti should be noticed that:

Cancerous formations are typically stiffer compared to the surrounding healthy soft tissues [30, 21]. Many tumor identification methods, for example, elastography, are based on this fact [26]. Tumors are also commonly modeled as homogeneous [7, 20, 34]. Therefore, we assume that the tumors are stiffer than the surrounding healthy soft tissues and they are homogeneous in this paper. However, the quantitative measurements of tumor stiffness suggest a wide variability between tumor types [25] and some tumors may have fat containing regions that appear less stiff [28]. The role of differential stiffness on tissue stiffness identification needs to be investigated in the future research.

In this paper, only finite element modeling was used to compare the deformation of different hyperelastic materials during indentation. Experimental data would be required to further confirm the results we acquired using finite element modeling in the future study.

In our method, a rolling indentation probe was used to palpate the soft tissue based on the assumption that a single probe might be enough to substitute bi-digital palpations [18, 34]. The comparison between probing and bi-digital palpations may need further investigation.

Most participants had no palpation experience in this study. Future study would involve participants with medical background even experienced surgeons.

5 Conclusions

A 3D pseudo-haptic feedback method is proposed to express haptic perception through a visual display. A low-cost combined pseudo-haptic feedback and force feedback method to enhance the perception of haptic feedback has been conceived, implemented and shown to be capable of identifying hard inclusions inside a soft tissue. The performance of the combination of the pseudo-haptic feedback and force feedback was comparable with the performance of the gold standard of manual interaction, which identifies hard nodules through a user's direct touch sensation. Compared to sole pseudo-haptic feedback or force feedback, the proposed combined feedback technique enabled participants to detect hard nodules in soft tissue more quickly. The survey showed that participants using the pseudo-haptic feedback combined with force feedback method had an enhanced experience of palpation perception. Our combined feedback method which has been evaluated to successfully augment haptic perception can find future applications in medical palpation simulators. We demonstrated the potential of our combined feedback method in medical simulators: a lot of work and effort and user studies remain to show how that this technique can be efficiently used in a real medical simulator

Acknowledgements The research leading to these results has received funding from the National Natural Science Foundation of China (approval no. 51175412), the China Scholarship Council, the GSTT charity, the National Institute for Health Research (NIHR) Biomedical Research Centre based at Guy's and St Thomas' NHS Foundation Trust and King's College London, and the European Commission's Seventh Framework Programme under grant agreement 287728 in the framework of EU project STIFF-FLOP. The views expressed are those of the authors and not necessarily those of the NHS, the NIHR or the Department of Health.

References

1. Altman DG, Bland J (1994) Diagnostic test 1: Sensitivity and specificity. BMJ 308:1552
2. Bibin L, Anatole L, Bonnet M, Delbos A, Dillon C (2008) SAILOR: a 3-D medical simulator of loco-regional anaesthesia based on desktop virtual reality and pseudo-haptic feedback. In: ACM Sysmposium on Virtual Reality Software and Technology (VRST) 2008, pp 97-100
3. Conover WJ (1980) Practical Nonparametric Statistics. 2nd ed., John Wiley & Sons, pp 225-226
4. Ernst MO, Banks MS (2002) Humans integrate visual and haptic information in a statistically optimal fashion. Nature 415(6870):429-33
5. Fawcett T (2006) An introduction to ROC analysis. Pattern Recognit Lett, 27(8):861-874
6. De Gersem G (2005) Reliable and enhanced stiffness perception in soft-tissue telemanipulation. The Int J of Robotics Res 24(10): 805-822
7. Gwilliam JC, Mahvash M, Vagvolgyi B, Vacharat A, Yuh DD, and Okamura AM (2009) Effects of haptic and graphical force feedback on teleoperated palpation. In: Proceedings of IEEE International Conference on Robotics and Automation 2009, pp 677682.
8. Hachisu T, Cirio G, Marchal M, Lcuyer A (2011) Pseudo-haptic feedback augmented with visual and tactile vibrations. In: IEEE International Symposium on Virtual Reality Innovation 2011, pp 327-328
9. Hayward V (2008) A brief taxonomy of tactile illusions and demonstrations that can be done in a hardware store. Brain Res Bulletin 75(6):742-52

10. Hayward V, Astley O, Cruz-Hernandez M, Grant D, Robles-De-La-Torre G (2004) Haptic interfaces and devices. Sensor Rev 24(1):16-29
11. Kim SY, Kyung KU, Park J, Kwon, DS (2007) Real-time area-based haptic rendering and the augmented tactile display device for a palpation simulator. Adv Robotics 21(9):961-981
12. Kimura T, Nojima T (2012) Pseudo-haptic feedback on softness induced by grasping motion. Isokoski P and Springare J (Eds.): EuroHaptics 2012, pp 202-205
13. Klatzky RL, Lederman SJ, Langseth S (2003). Watching a cursor distorts haptically guided reproduction of mouse movement. J of Exp Psychol: Appl 9(4):228-235
14. Lecuyer A, Burkhardt JM, Coquillart S, Coiffet P (2001) Boundary of illusion: an experiment of sensory integration with a pseudo-haptic system. In: Proceedings of the 2001 IEEE Virtual Reality Conference, pp 115-122
15. Lecuyer A, Burkhardt JM, Tan CH (2008) A study of the modification of the speed and size of the cursor for simulating pseudo-haptic bumps and holes. ACM Trans on Appl Percept 5(3):1-21
16. Li M, Liu H, Seneviratne LD, Althoefer K (2012) Tissue stiffness simulation and abnormality localization using pseudo-haptic feedback. In: IEEE International Conference on Robotics and Automation 2012, pp 5359-5364
17. Li M, Faragasso A, Konstantinova J, Aminzadeh V, Seneviratne LD,Dasgupta P, Althoefer K (2014) A novel tumor localization method using haptic palpation based on soft tissue probing data. In: IEEE International Conference on Robotics and Automation. IEEE Robotics and Automation Society, Piscataway, USA, pp 4188-4193
18. Liu H, Li, J, Song X, Seneviratne LD, Althoefer K (2011) Rolling indentation probe for tissue abnormality identification during minimally invasive surgery. IEEE Trans on Robotics 27(3):450-460
19. Liu H, Noonan DP, Challacombe BJ, Dasgupta P, Seneviratne LD, Althoefer K (2010) Rolling mechanical imaging for tissue abnormality localization during minimally invasive surgery. IEEE Trans on Biomed Eng 57(2):404-14
20. Liu H, Sangpradit K, Li M, Dasgupta P, Althoefer K, and Seneviratne LD (2014) Inverse finite-element modeling for tissue parameter identification using a rolling indentation probe. Med Biol Eng Comput 52(1):17-28
21. Masuzaki R, Tateishi R, Yoshida H, Sato T, Ohki T, Goto T, Yoshida H, Sato S, Sugioka Y, Ikeda H, Shiina S, Kawabe T, and Omata M (2007) Assessing liver tumor stiffness by transient elastography. Hepatol Int 1(3):394-397
22. Mensvoort K, Vos P, Hermes DJ, Liere RV (2010) Perception of mechanically and optically simulated bumps and holes. ACM Trans on Appl Percept 7(2):10:1-24
23. Nakao Megumi, Kuroda T, Komori M, Oyama H (2003) Evaluation and user study of haptic simulator for learning palpation in cardiovascular surgery. In: International Conference on Artificial Reality and Telexistence 2003, pp 203-208
24. Nedel LP, Thalmann D (1998) Real-time muscle deformations using mass-spring systems. In: Proceedings Computer Graphics International 1998, IEEE Computer Society, Washington, DC, USA, pp 156-165
25. Netti PA, Berk DA, Swartz MA, Grodzinsky AJ, and Jain RK (2000) Role of extracellular matrix assembly in interstitial transport in solid tumors, Cancer Res 60(9):2497-2503
26. Salomon G, Kollerman J, Thederan I, Chun FKH, Budaus L, Schlomm T, Isbarn H, Heinzer H, Huland H, and Graefen M (2008) Evaluation of Prostate Cancer Detection with Ultrasound Real-Time Elastography: A Comparison with Step Section Pathological Analysis after Radical Prostatectomy. Eur Urol 54(6):1354-1362
27. Sangpradit K, Liu H, Dasgupta P, Althoefer K, Seneviratne LD (2011) Finite-element modeling of soft tissue rolling indentation. IEEE Trans on Biomed Eng 58(12):3319-3327.
28. Venkatesh SK, Yin M, Glockner JF, Takahashi N, Araoz PA, Talwalkar JA, and Ehman RL (2008) MR elastography of liver tumors: preliminary results. AJR Am J Roentgenol, 190(6):1534-1540.
29. Wallis S (2013) Binomial Confidence Intervals and Contingency Tests: Mathematical Fundamentals and the Evaluation of Alternative Methods. J. of Quant Linguist, 20(3), pp 178-208.
30. Wellman P and Howe R (1999) Breast tissue stiffness in compression is correlated to histological diagnosis. Harvad BioRobitics Lab Tech Rep

31. Wilcoxon F (1946) Individual comparisons of grounded data by ranking methods. J Econ Entomol 39:269
32. Wilson EB (1927) Probable inference, the law of succession, and statistical inference. J of Am Statistical Assoc 22:209-212
33. Woodward W, Strom E, Tucker SL, McNeese MD, Perkins GH, Schechter NR, Singletary SE, Theriault RL, Hortobagyi GN, Hunt KK, Buchholz T (2003) Changes in the 2003 American Joint Committee on Cancer staging for breast cancer dramatically affect stage-specific survival. J Clin Oncol 21(17):324-348
34. Yamamoto T and Abolhassani N (2012) Augmented reality and haptic interfaces for robotassisted surgery. Int J Med Robot Comput Assist Surg 8:45-56.
35. Yau C (2009) R tutoral eBook. r-tutor.com. http://www.r-tutor.com/elementary-statistics/non-parametric-methods/wilcoxon-signed-rank-test Accessed 20 Mar 2014

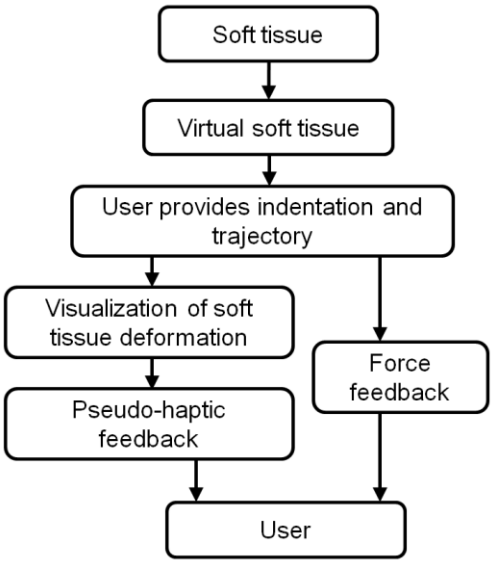

Fig. 1 The flowchart of the combined pseudo-haptic and force feedback for soft object interaction

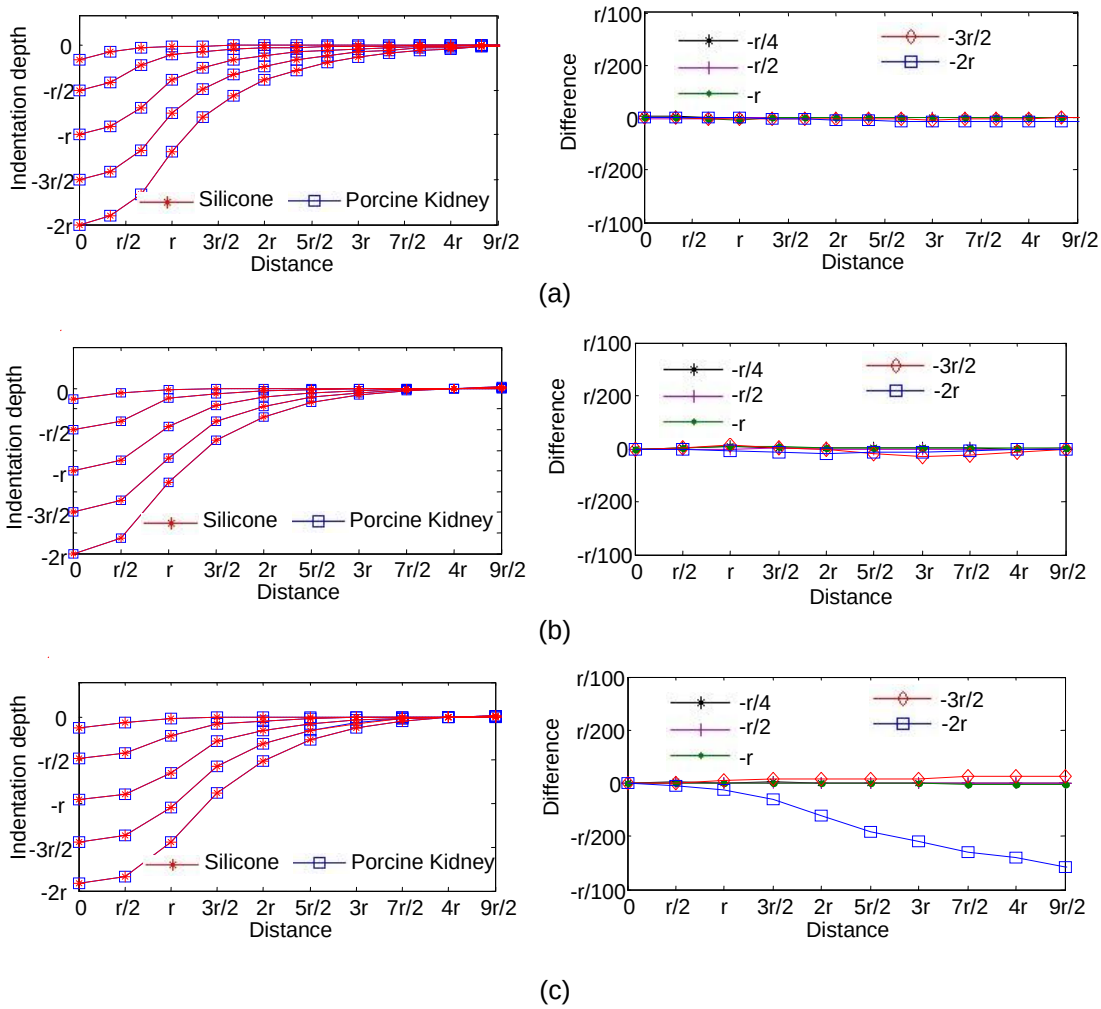

Fig. 2 On the left panels the deformation curvature of silicone (RTV6166 gel) and porcine kidney at different indentation depths are reported, by using 6mm (a), 8mm (b), and 10mm (c) indenter, according to 3D finite element simulation; on the right panels the difference between the displacement curvatures are reported

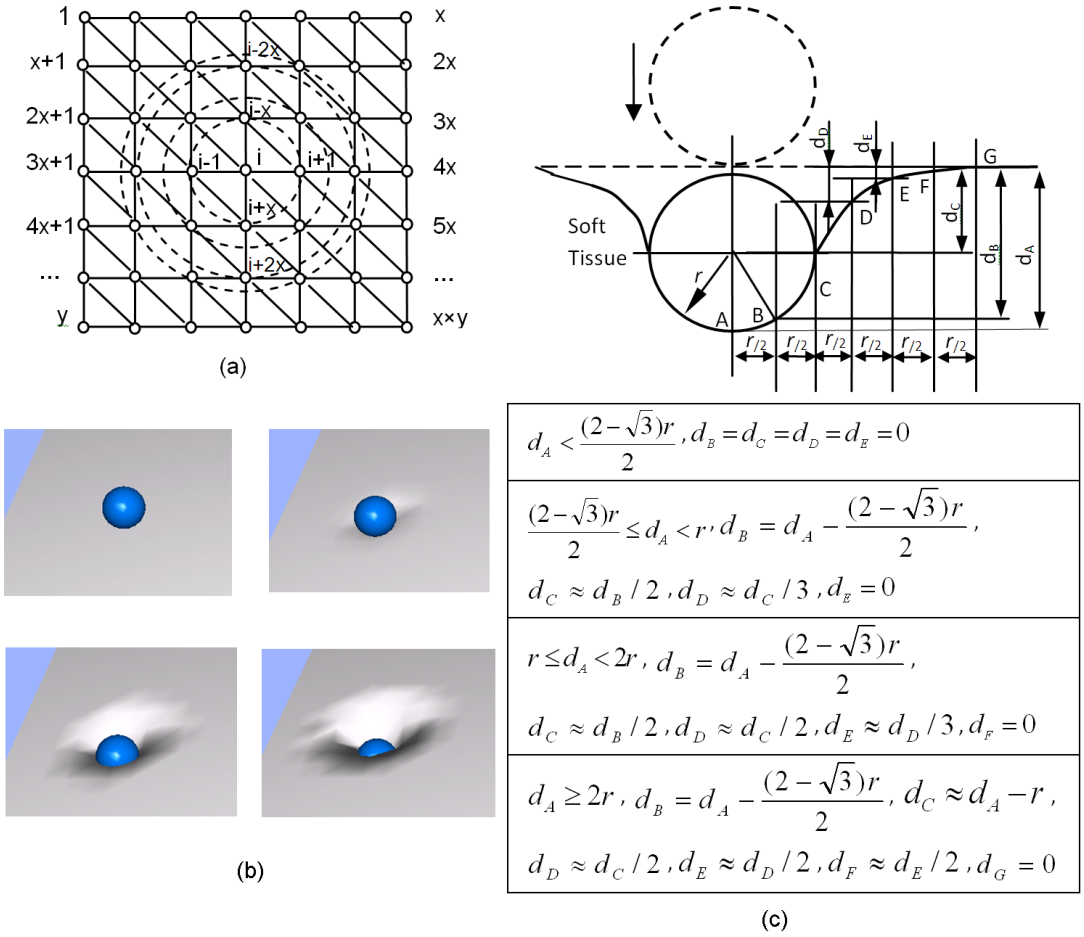

Fig. 3 (a) Mesh representation for the soft object deformation visualization: the number of the vertices of triangles of soft object surface is $x \times y$, where the node i is positioned at the center of the indentation area; (b) tissue deformation increases as indentation depth increases; (c) simplified model of deformation curvature of soft tissue surface

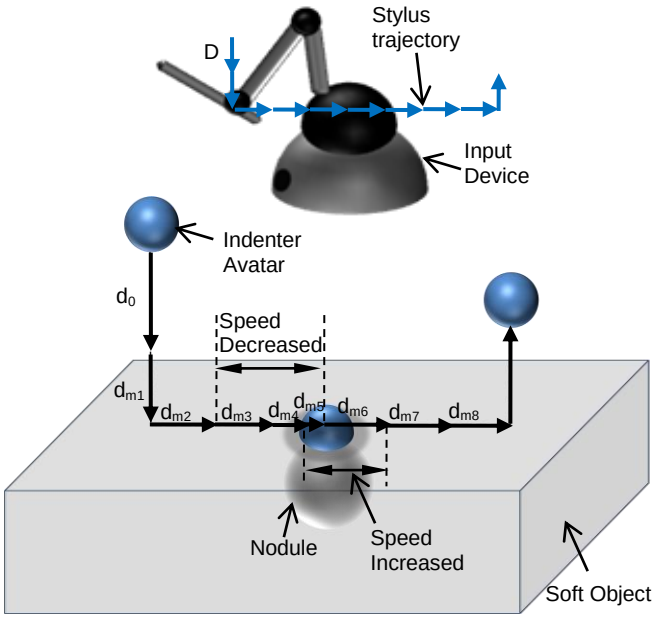

(a)

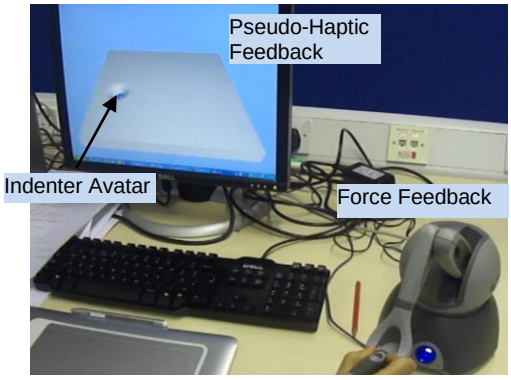

(b)

Fig. 4 (a) Modification of the cursor speed when passing over a hard nodule; (b) combined force feedback and pseudo-haptic feedback.

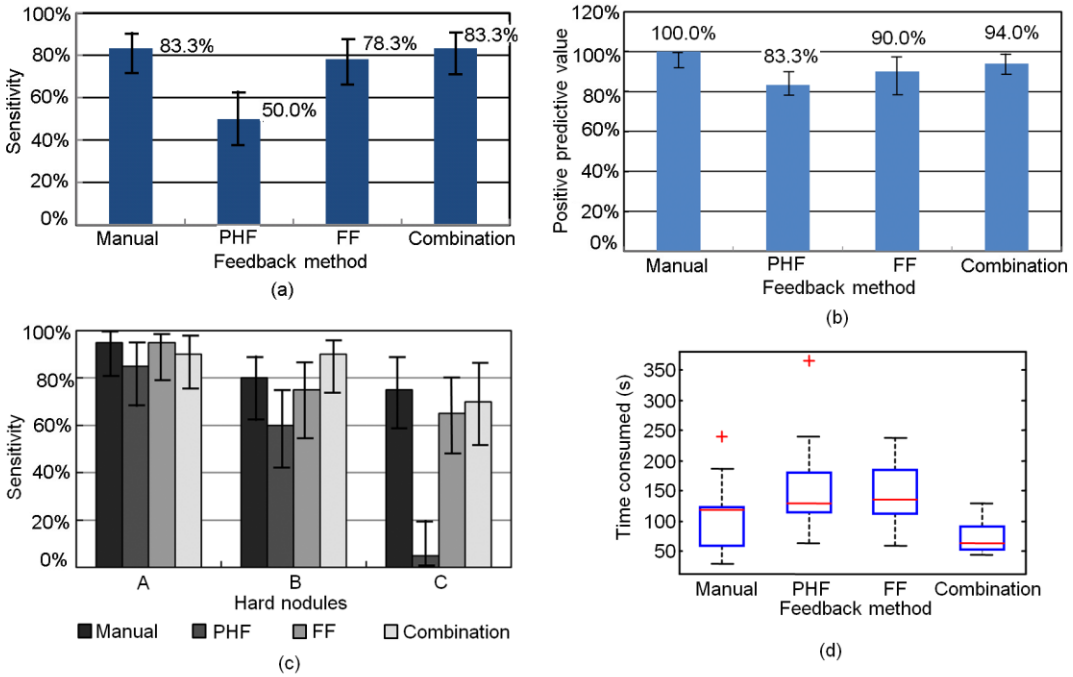

Fig. 5 (a) Nodule detection sensitivities of nodule A, B, and C with Wilson score intervals at a 95% confidence level; (b) overall nodule detection sensitivities with Wilson score intervals at a 95% confidence level; (c) positive predictive values with Wilson score intervals at a 95% confidence level; (d) time needed to find nodules using manual palpation, PHF, FF and combination technique of PHF and FF

Explorative Condition	Equation for Displacement Distance
Indentation depth is increasing (Δf_n>0)	$d_m(z) = R_n \cdot D(z)$
Indentation depth is decreasing (Δf_n<=0)	$d_m(z) = R_o \cdot D(z)$
Soft tissue stiffness in current position is stiffer than the tissue in the previous position (Δf_n>0)	$d_m(x,y) = R_h \cdot D(x,y)$
Soft tissue in current position has the same stiffness or softer than in the previous position (Δf_n<=0)	$d_m(x,y) = R_o \cdot D(x,y)$

Table 1 Algorithm of the 3D pseudo-haptic feedback for intra-operative hard nodule identification

	Item	*CI*	*Δp*	Significance?
Se	Manual & FF	0.142	0.050	No
	Manual & PHF	0.167	0.333	**Yes**
	Manual & Combination	NULL	NULL	No
	FF & PHF	0.171	0.283	**Yes**
	FF & Combination	0.142	0.050	No
	PHF & Combination	0.167	0.333	**Yes**
PPV	Manual & FF	0.090	0.100	**Yes**
	Manual & PHF	0.113	0.167	**Yes**
	Manual & Combination	0.081	0.060	No
	FF & PHF	0.142	0.067	No
	FF & Combination	0.071	0.040	No
	PHF & Combination	0.098	0.107	**Yes**

Table 2 Comparison of nodule detection sensitivities and positive predictive values in the tests of combined pseudo-haptic and force feedback

Item	n_r	W	$W_{critical}$	Significance
Manual & FF	19	42	46	**$W < W_{critical}$, Yes**
Manual & PHF	18	22	40	**$W < W_{critical}$, Yes**
Manual & Combination	19	47.5	46	$W > W_{critical}$, No
FF & PHF	20	99.5	52	$W > W_{critical}$, No
FF & Combination	19	6	46	**$W < W_{critical}$, Yes**
PHF & Combination	19	4	46	**$W < W_{critical}$, Yes**

Table 3 Wilcoxon signed-rank tests for consumed time